VOLATILES INVESTIGATING POLAR EXPLORATION ROVER (VIPER) THERMAL MANAGEMENT SYSTEM (TMS) DESIGN, DEVELOPMENT, AND TESTING

Joshua Smay, Jimmy Hughes, Ryan Spangler, and Calin Tarau
Advanced Cooling Technologies, Lancaster, PA, 17601

Angel R. Alvarez-Hernandez
NASA Johnson Space Center, Houston TX 77058

ABSTRACT

The Volatiles Investigating Polar Exploration Rover (VIPER) Thermal Management System (TMS) is a critical part of the vehicle's thermal subsystem that ensures rover electrical components are maintained within operational and survival limits. NASA performed a trade study in 2019 for various technologies to define the VIPER TMS concept. The Loop Heat Pipe (LHP) with Thermal Control Valve (TCV), was selected in 2021 as the main transport component for flight after completion of the Thermal Vacuum (TVAC) testing for initial study. This initial study also defined the warm-box design as honeycomb panels with embedded constant conduction heat pipes. These early efforts defined the final VIPER TMS and the requirements needed in SBIR contracts to ACT for flight hardware. The VIPER TMS concept was designed to meet challenging thermal requirements, which included extended operations in Permanently Shadowed Regions (PSRs) and extended lunar darkness survival. The VIPER TMS intended to minimize heat loss during lunar darkness to optimize power consumption, and to maximize heat rejection during maximum thermal loading. The components under contract included a warm-box, for the temperature sensitive electronics to reside, the thermal transport design four Loop Heat Pipes, and the radiator panel assembly with Z93C55 white coating. Additionally, axial grooved constant conductance heat pipes are used to thermally couple each side of the warm-box, and to couple the MSOLO and NIRVSS science instruments, located outside of the warm-box, to the warm-box environment. One of the key innovations was to incorporate passively activated Thermal Control Valves (TCV) into the LHPs to reduce heat loss during lunar darkness operations. This NASA and ACT collaboration resulted in the successful final design, manufacturing and delivery of the TMS flight components to Johnson Space Center for vehicle integration. This publication captures the work performed to meet the thermal requirements and the component level testing performed.

NOMENCLATURE, ACRONYMS, ABBREVIATIONS

R Thermal Resistance (K/W)

Q Heat Rate (W)

INTRODUCTION

The volatiles Investigating Polar Exploration Rover (VIPER) is a roughly 1.5 meter cube sized lunar rover that will be used to survey and prospect the south pole of the moon in search of frozen water. This mission will require VIPER to delve into permanently shadowed regions (PSRs) repeatedly and survive multiple cycles of lunar darkness.

The VIPER TMS has to meet unprecedented thermal environments for its mission. Some of the thermal environments it is designed for are; Surviving extended hibernation in lunar darkness, and operating for extended periods surviving the missions worst case hot operating conditions, while maintaining all components within temperature limits.

The resultant system dissipates energy efficiently during lunar day when electronics are at maximum dissipation while safeguarding residual energy during lunar night, when each Watt of energy lost requires 5 kilograms of batteries to sustain.

ARCHITECTURE

The thermal architecture strategy is to centralize the heat within the rover for transport to the radiator panels. This is achieved by utilizing a “warm-box”: a thermally isolated box constructed of honeycomb panels that houses temperature-sensitive, mission-critical electronics. The box is isolated via mounting to the frame through non-conductive plastic (Ultem) and multi-layer insulation (MLI) coverage. Waste heat from the electronics is gathered in the warm-box and transported, via aluminum-ammonia Constant Conductance Heat Pipes (CCHPs) embedded in the honeycomb panels to the evaporator of four Loop Heat Pipe (LHP) evaporators – one affixed to each side of the warm-box. CCHPs are passive two-phase heat transfer devices with extensive flight heritage that transport heat effectively with a low temperature gradient from the heat input area, or evaporator, to the heat rejection area, or condenser, by utilizing the working fluid (ammonias) latent heat. Heat input causes the fluid to boil, send vapor to the condenser, condense, and then return to the evaporator through the axial groove wick by a small amount of capillary action and, if the condenser is above the evaporator (reflux orientation), gravity. The LHPs are plumbed with a passive thermal control valve (TCV) that will either send vapor generated in the evaporator to the radiator panels for dissipation or back to the compensation chamber, effectively shutting down the two-phase heat transport capability of the LHPs passively. CCHPs in reflux orientation were mounted to the external surfaces of the warm-box; these serve to share uneven heat loads between adjacent walls of the warm-box and are designed to provide redundancy such that the rover could continue operating if one LHP were to fail. These CCHPs are referred to as the Crossing, External, or Connecting CCHPs. To maintain the same thermal transport from electronics to radiator panels, two external instruments are also linked to the warm-box using refluxing CCHPs, referred to as the Instrument CHPs. CAD renderings of the TMS are seen in Figure 1 below, and sub-sections of each component/sub-assembly of the TMS are explained in further detail in the following sections.

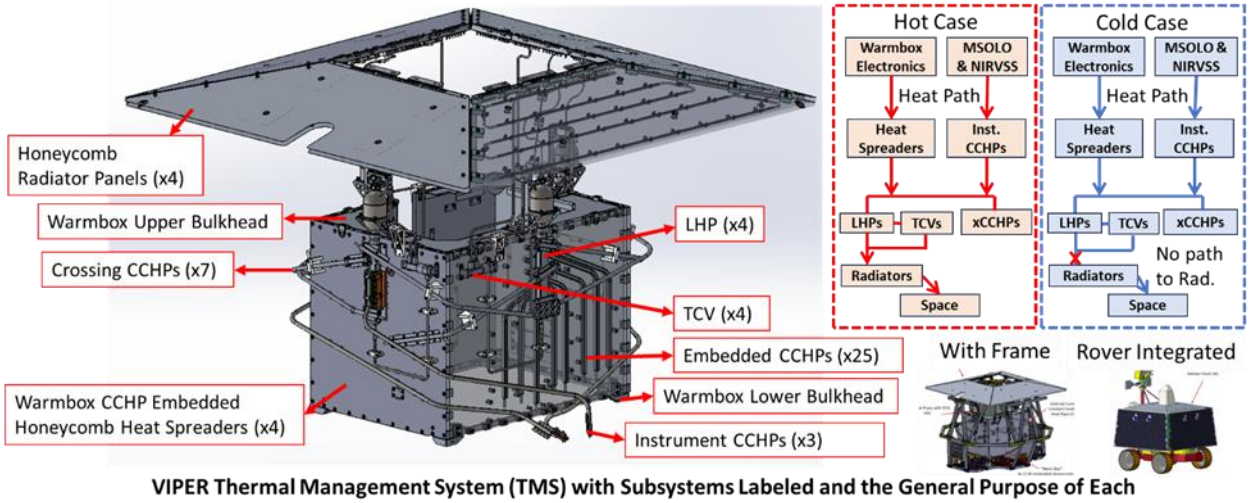

Figure 1. CAD Renderings of VIPER Rover Highlighting TMS Components

Warm-Box with External Connecting CCHPs

The warm-box serves as a thermally isolated housing for critical and temperature-sensitive electronics. It comprises of four CCHP-embedded honeycomb heat spreaders (the "walls"), a machined lower bulkhead, and a folded sheet metal upper bulkhead. The bulkheads provide rigidity and strength to the box, an electric grounding path from the walls to the remainder of the rover, keep the box square, and allow the TRIDENT (The Regolith and Ice Drill for Exploring New Terrains) drill – a 1 meter drill that passes through the center of the rover – to have unimpeded access to the lunar regolith via large cutouts. The warm-box was designed to be thermally isolated from the rover structure and heavily insulated using Multi-Layered Insulation (MLI) such that the only heat transport – thus, possible heat leak path – from the warm-box to the radiator panels was by way of the four LHPs with TCVs. Figure 2 shows the fully assembled warm-box at NASA Johnson Space Center (JSC).

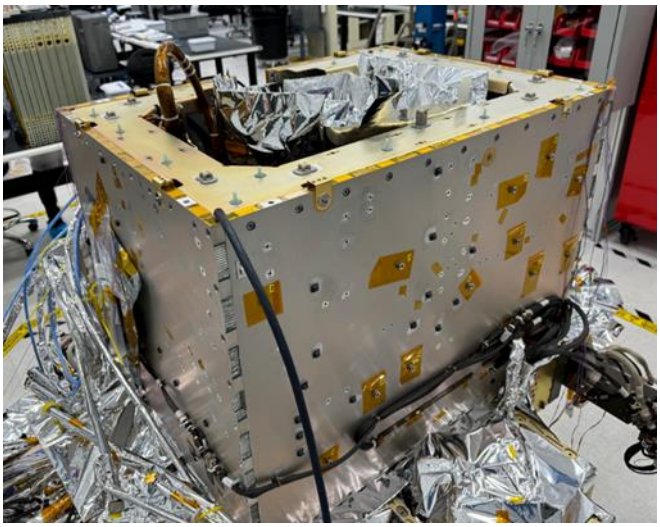

Figure 2. Fully assembled warm-box at NASA Johnson Space Center (JSC)

The primary thermal control device of the warm-box lies within the honeycomb panels that comprise the walls of the assembly. Aluminum-ammonia CCHPs are strategically routed to gather relevant waste heat from the electronics mounted to the internal surfaces of the walls and transport the heat to the LHP evaporators. Due to the operating principles of CCHPs explained above, generally, there exists less than 5°C temperature difference between the source and the LHP evaporator. The CCHPs use the traditional axial groove wick structure designed to minimize pressure drops experienced in micro-gravity operating environments. However, this wick structure is not able to wick against gravity (evaporator over condenser) as the pore radius is too large to overcome any meaningful hydrostatic pressure. Therefore, CCHPs were designed to always be in a refluxing orientation (condenser over evaporator), including the consideration of a maximum 15° rover tilt, to take advantage of the lunar gravity to assist liquid return from the condenser to the evaporator. Routing of the CCHPs avoided embedded inserts that serve as mounting points for internal electronics, external LHP evaporators, and External Connecting CCHPs.

External Connecting CCHPs span between adjacent warm-box heat spreader walls to share heat loads and bring the system closer to thermal equilibrium. Like the embedded heat spreader CCHPs, the External Connecting CCHPs use a traditional axial groove wick structure. Efforts were made to route the CCHPs such that they were always refluxing regardless of rover tilt, and to place the evaporators and condensers of the CCHPs directly on the respective LHP evaporators to produce the optimal thermal connection; however, due to geometry restrictions, this was not physically possible. Certain rover tilts would result in small adverse gravity orientations along short portions of the overall routing. Each case that could operate in adverse gravity head was evaluated and determined to have positive capillary pressure margin over the minimal hydrostatic pressure that was generated – this was primarily possible due to the weakened gravitational acceleration on the Moon, which is 1/6th that present on Earth. Additionally, several CCHP evaporators needed to be directly mounted to the external surface of the heat spreader in lieu of the LHP evaporator due to geometry restrictions; this adjusted mounting relies on the heat spreader embedded CCHPs to bring the energy to the external CCHP evaporator, rather than pulling the heat directly from the LHP evaporator itself.

Instrument CCHPs

Three refluxing CCHPs were used to bring waste heat directly from instruments (two attached to the MSOLO, Mass Spectrometer Observing Lunar Operations, and one attached to the NIRVSS, Near-Infrared Volatiles Spectrometer System), located externally of the warm-box, to the LHPs mounted on the external surfaces of the warm-box; this was done to maintain the principle of biasing all heat rejection through the four LHPs with TCVs. These instrument CCHPs were constructed using the traditional axial groove wick structure extrusions and, thus, had similar operating constraints to the embedded heat spreader CCHPs and external connecting CCHPs. The routing of each CCHP put them into a refluxing orientation at nominal rover stance, with best effort to keep the long, bending routing of each CCHP in a gravity-assisted inclination at worst-case rover tilts. Each CCHP went to a separate LHP to maintain balance on the magnitude of dissipations serviced by each loop.

The instrument CCHPs were a late addition to the overall system architecture; the result of which was non-ideal mounting approaches, materials, and interfaces that ate up much of the thermal resistance budget available from the instruments to the LHPs. A nominally charged – i.e. charged as a normal CCHP would be, such that the grooves would be fully filled in micro-gravity – CCHP would result in an excessively heavy fluid volume, an issue that compounds the longer the CCHP is. This heavy charge would result in transient start-up spikes, as the vapor needs to superheat to displace the fluid column, excess fluid that would increase the resistance into the vapor, and the transition from natural convection in the fluid pool to nucleate boiling, further eating into the budget. Additional optimization to determine the minimum fluid needed to dissipate the waste heat while minimizing transient start-up spikes was completed and determined to be sufficient to meet the resistance requirements from the instruments to the LHPs. CAD renderings of the Instrument CCHPs are shown in Figure 1.

LHPs with TCVs and Radiator Panels

Four LHPs with TCVs are used to couple thermally the warm-box to the radiator panels located at the top of the rover. The evaporators were attached to the external surfaces of the warm-box heat spreader walls – each heat spreader had one LHP equipped to act as the primary transport mechanism for waste heat dissipation for electronics affixed to the interior surface of each respective warm-box wall. Throughout development, it was determined that the stronger the thermal coupling of the TCV to the temperature(s) the LHP evaporators was, the more responsive the TCV was to actuate; effectively, the vapor traveling through the TCV would need to overcome the thermal mass of the TCV itself and whatever the valve was attached to. To minimize the effect, the valves were also mounted to the same heat spreader the LHP evaporator was attached to.

Traditional LHPs consist of the pump body (the subassembly consisting of the primary and secondary wick structures, the evaporator body, the compensation chamber, and associated internal components), vapor and liquid transport lines, and condenser tubing. The LHP operates by a pressure (temperature) differential between the evaporator body and the compensation chamber. A seal at the connection of the evaporator to compensation chamber prevents vapor generated in the evaporator from being able to go directly “back” to the compensation chamber; thus, the vapor must travel through the vapor transport line, through the condenser (where it condenses back to liquid), and through the liquid transport line to the compensation chamber. A schematic of typical LHPs is shown in Figure 3.

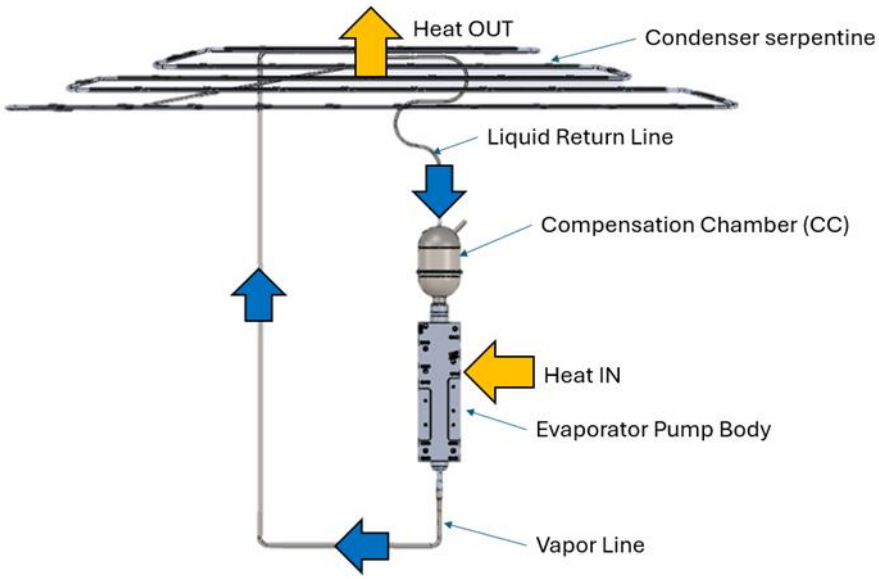

Figure 3. Schematic of typical LHP

The functional performance by way of a pressure differential between evaporator and compensation chamber provides a tried-and-true mechanism for shutting down the LHP, or canceling the pressure differential and, thus, the two-phase flow. A small (<5W) heat load applied to the compensation chamber can increase the temperature to match the evaporator temperature, effectively bringing the pressure differential to zero and stopping flow. An improvement to this traditional approach was desired for VIPER for the following reasons:

- Requiring a heat load on the compensation chamber to shut the LHP down, while only a few Watts, is additional energy that would need to be stored and discharged by several kilograms of batteries per Watt. This energy storage would be additional to the typical heat leaks that occur via conduction and radiation that need to be compensated for using survival heaters at the electronics.
- Transport lines from the evaporator to the condenser would be unimpeded by any physical barriers. Operation in a gravity environment and orientation (condenser above the evaporator) could induce single- or two-phase flows driven by consequences of alternate physics than those traditional of a LHP – e.g. Single-phase flow driven by density differences and/or two-phase thermosyphon flow as the free surface of the working fluid has a view factor to the condenser.

These considerations, supported by Engineering Demonstration Unit test results, led to LHPs with TCVs being the selected transport mechanisms. This LHP configuration is constructed in largely the same manner and operates using the same pressure-driven flow principles, but a TCV is plumbed into the transport lines; the vapor line is welded to the TCV and two outlets – one routed to the condenser and one, called the bypass, is routed back into the compensation chamber – complete the fluid circuitry. The TCV actuates as a function of temperature. When the system

is warm and energy needs to be dissipated, the TCV directs vapor flow to the condenser where the energy can be dissipated to space. When the system is cold and the rover wants to store residual energy, the TCV directs any two-phase flow back to the compensation chamber of the system. Flow through the bypass line keeps energy within the pump body/warm-box subsystem and has the benefit of heating the compensation chamber, which reduces the potential generated by the system to create a two-phase flow. An image demonstrating normal operation (flow to condenser) and bypass mode (flow to compensation chamber) is shown in Figure 4.

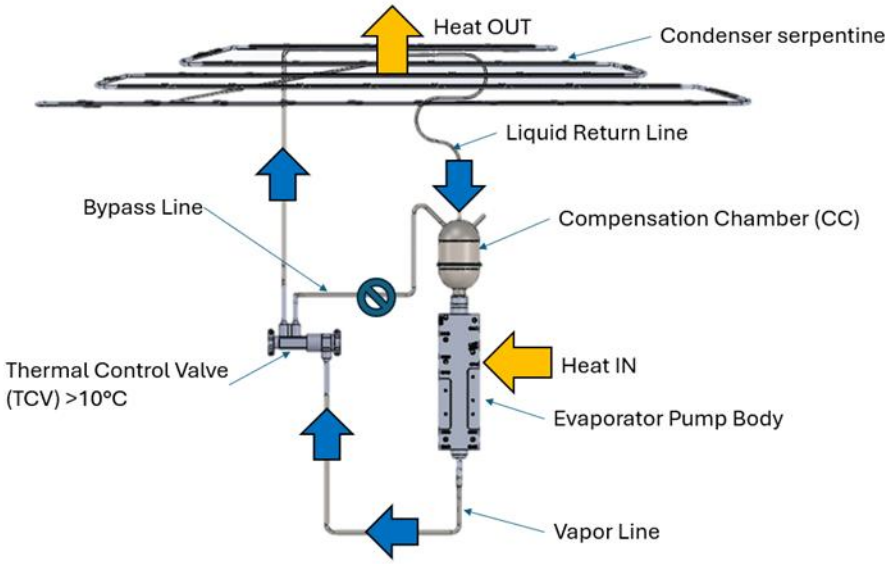

Figure 4. LHP with TCV for Bypass

The condenser of the LHPs are attached to the inside surfaces of trapezoidal honeycomb radiator panels; each LHP condenser is attached to a single radiator panel. The radiator panels are traditional aluminum honeycomb construction and sized to dissipate worst-case energy dissipations at maximum effective sink temperature with margin; external surfaces are painted with Z93C55 white emissive paint and arranged into a partial pyramidic configuration. An image of the LHPs with TCVs and radiator panels attached to the rover assembly is shown in Figure 5.

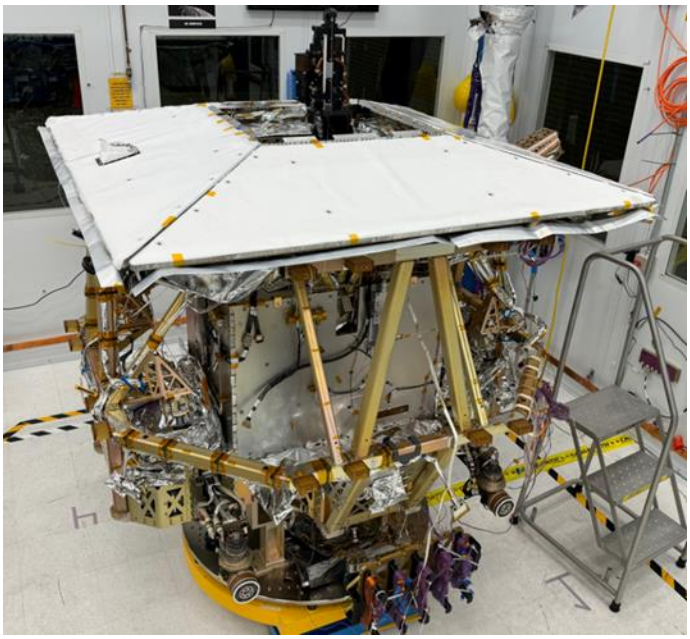

Figure 5. LHPs with TCVs and Radiator Panels Attached to Rover During Assembly

ANALYSIS

All major components of the system were analyzed to some extent during the program's design portion. The analyses performed by ACT included the following. First, the LHPs across the rover were sized based on their required power transport and thermal conductance. These LHP performance calculations were validated with an Engineering Demonstration Unit (EDU) LHP that was built and tested early on in the program's life cycle. Once, validated, minor updates to the LHP design/analysis were made to confirm the sizing and performance would be adequate for the flight LHPs. Second, using the confirmed LHP sizing, the heat spreader panels with embedded CCHPs were analyzed to finalize the internal CCHP layout/routing and verify the heat spreading/transport capability of the panels. The goal of the heat spreader analysis was to close on a design that kept the components mounted to them under the maximum temperature limits, with margin. The secondary goal was to maintain a low thermal gradient across the panel. Third, a quarter model of the main components of the TMS – the port Heat Spreader, the port LHP, and the port Radiator Panel were analyzed to confirm sufficient performance at a higher assembly level. Lastly, the CCHPs and the Instrument CCHPs were analyzed for thermal conductance.

As mentioned, the first system analyzed/designed for the program was the LHP. The inputs of the calculations are the main design parameters including geometry and material, while the main outputs are the overall thermal conductance of the LHP and a plot showing the design's capillary limit and system pressure drop vs operating temperature. Using the mission's requirements for conductance and power transport capability, the LHP could thus be designed and analyzed for the mission. Figure 6 shows the final flight design's output pressure drop and capillary limit curve. This design had an overall thermal conductance of approximately 20 W/K. While most of the input/design parameters are proprietary, the materials include an aluminum 6061 evaporator body, with a sintered nickel wick and propylene working fluid.

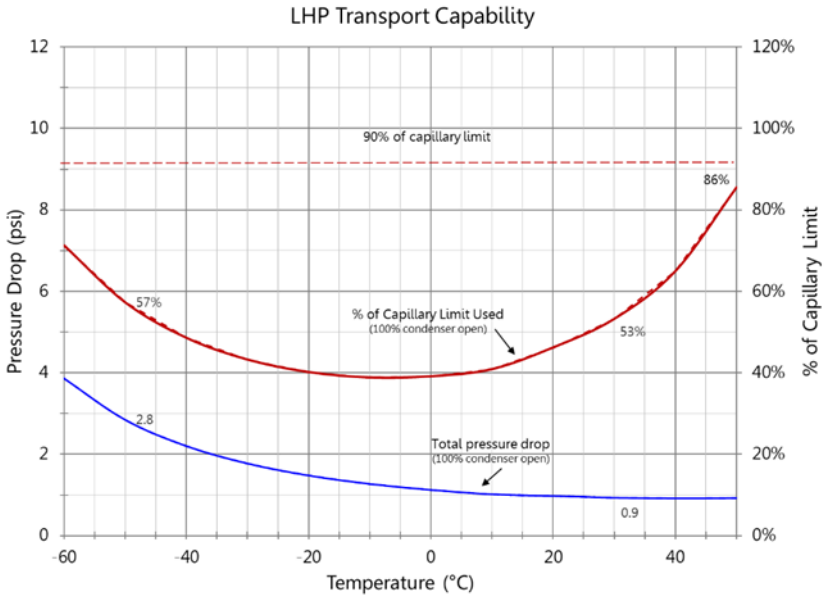

Figure 6. LHP Transport Capability

The LHP analyses mainly consisted of estimating the pressure drop across the LHP, and then using a thermal resistance network to estimate the steady state conductance. First, the maximum capillary limit for the LHP is calculated based on the working fluid properties and wick design. Next, the mass flow rate is calculated using the heat input to the evaporator and the working fluid properties. Once the mass flow rate is calculated, the pressure drop across the vapor lines, liquid lines, vapor grooves, and condenser can be calculated using various correlations including the Lockhart-Martinelli correlation1 for the two-phase transition in the condenser.

The conductance of the LHP is calculated using a thermal resistance network pictured below in Figure 7.

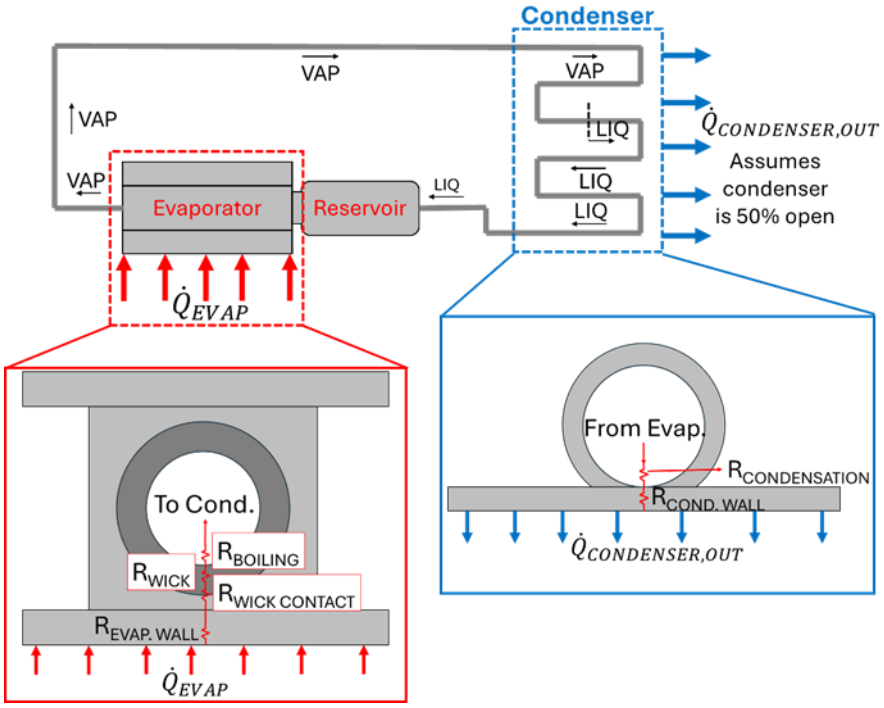

Figure 7. LHP Thermal Resistance Network

As mentioned, the EDU portion of the program included validation of these LHP calculations. During this exercise, the difference between the estimated and tested conductance was approximately 16%, resulting likely from conservative assumptions of the model.

With the LHP sized appropriately for the mission, it was then possible to take that evaporator body footprint, along with the electronics component footprints and layouts, and design and analyze the embedded CCHP Heat Spreader honeycomb panels. The analysis of the Heat Spreaders was done using a “conduction” model. Figure 8 below illustrates the modeling approach taken for the Heat Spreader analysis.

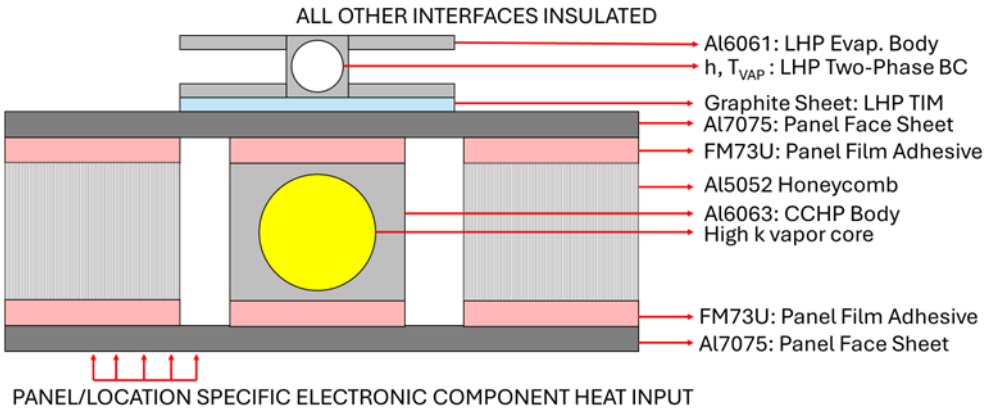

Figure 8. Heat Spreader Modeling Approach

The boundary condition of the LHP was modelled as a heat transfer coefficient applied to the bore of the LHP with a heat transfer coefficient obtained from testing data of the EDU LHP. The reference temperature of the convection boundary condition for the LHP was then representative of the vapor temperature of the LHP, and it was adjusted to obtain an average temperature across the evaporator body interface of 30°C: the hot case operational point. The LHP evaporator body, made of aluminum, was then connected to the honeycomb panel face sheet through a contact resistance equivalent to the planned graphite sheet thermal interface material (TIM). The honeycomb panels consisted of aluminum face sheets connected to both the heat pipes and the aluminum core through a contact resistance equivalent to the planned FM73U film adhesive. The embedded CCHPs, despite having two-phase heat transfer within them, were modeled as an aluminum envelope with a high conductivity core to simulate the two-phase operation. This is a standard approach used by ACT for FEA of heat pipes. All other surfaces were assumed insulated, i.e. covered with MLI. The discrete heat loads for each component were applied directly to the face sheet over the component footprint area and location. To account for the heat input being applied directly to the face sheet, the analysis and embedded heat pipe layout/design was completed with the goal of keeping the component footprints' max temperatures below the limit including a 5°C margin. The 5°C margin was an assumed temperature difference from the face sheet, through the component's thermal interface material, and to the location of the temperature limit for the component. Lastly, the CCHP layout inside the panel was adjusted until the component max temperature requirements including the 5°C margin was met. Figure 9 below shows the final analysis results for the port Heat Spreader Panel.

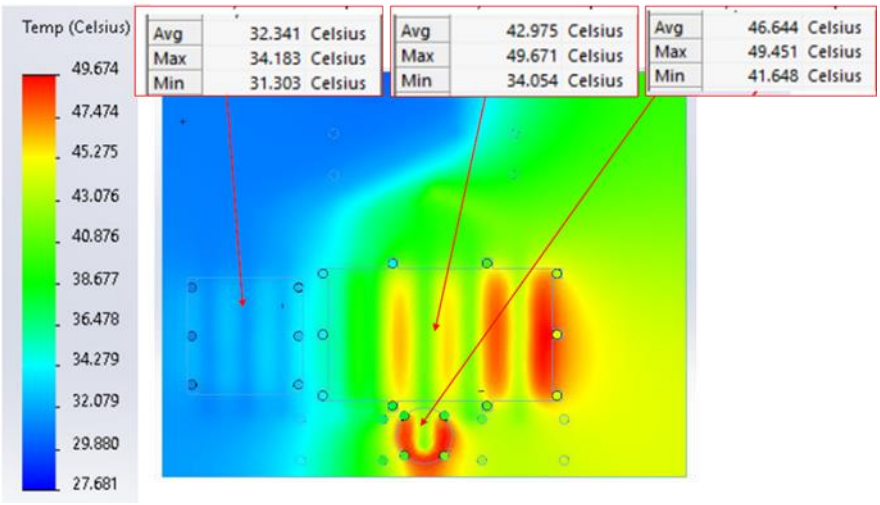

Figure 9. Heat Spreader Thermal Gradient During Hot Operation

With the Heat Spreaders and LHPs now designed and analyzed, it was possible to complete a subassembly model analysis of a quarter of the entire TMS. This subassembly analysis was completed for the steady state hot case, and included the port Heat Spreader panel, the corresponding LHP, and a model of the Radiator Panel. Furthermore, this analysis included radiative heat transfer. The Radiator Panel was modeled similar to the Heat Spreader in terms of construction, with the main difference being the lack of any embedded heat pipes. Some other differences of the radiators include less dense aluminum core and a radiative boundary condition for the outer face sheet, with radiator properties equivalent to Z93-C55 paint. The boundary conditions of the model include a representative space sink temperature which would take into account earth IR, lunar reflections, etc., an internal sink temperature, and the same 3 heat inputs to the Heat Spreader as in the previous analysis above. Figure 10 below shows the final results of the subassembly analysis.

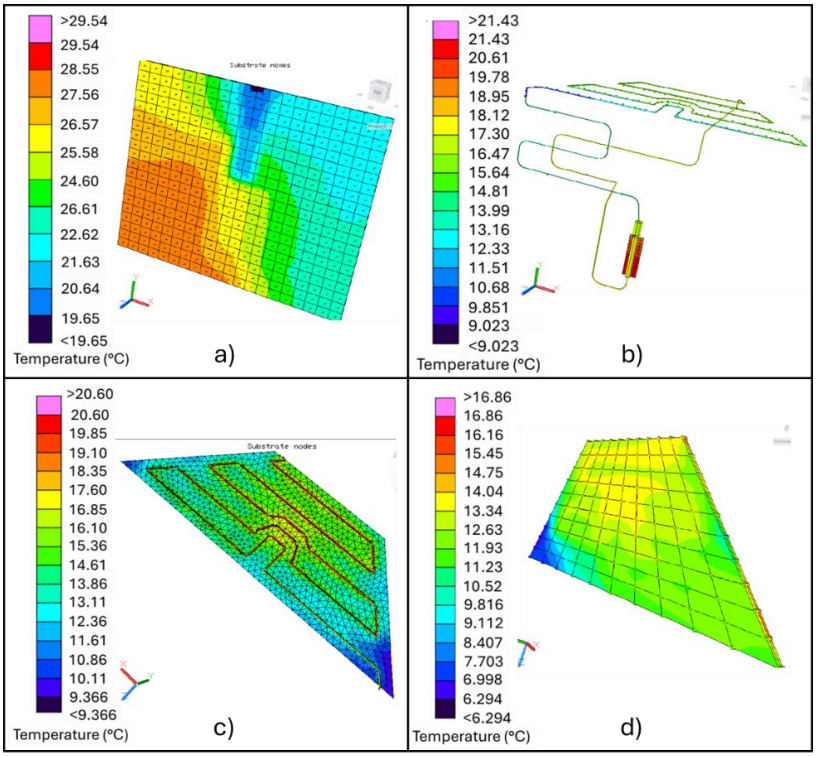

Figure 10. a) Heat spreader, b) LHP, c) Radiator - LHP side, d) Radiator - Space side in Thermal Desktop

Lastly, the connecting CCHPs (xCCHPs) and Instrument CCHPs were analyzed using a thermal resistance network pictured in Figure 11. The design of the xCCHPs was largely driven by the pre-determined LHP evaporator body width – which restricts the evaporator and condenser lengths – and the need for the xCCHPs to be gravity-aided despite a 15 degree rover tilt in any direction. The CCHPs are modelled here as a conductance per length for the evaporator and condenser. The conductance per length values were obtained from past test data for the representative extrusion. Table 1 below shows an example of the resistance network and dT calculations for the pipe highlighted in blue in Figure. All xCCHPs and the Instrument CCHPs, were analyzed in this manner. The construction of the CCHPs were nearly identical to the xCCHPs in terms of materials and CCHP extrusion.

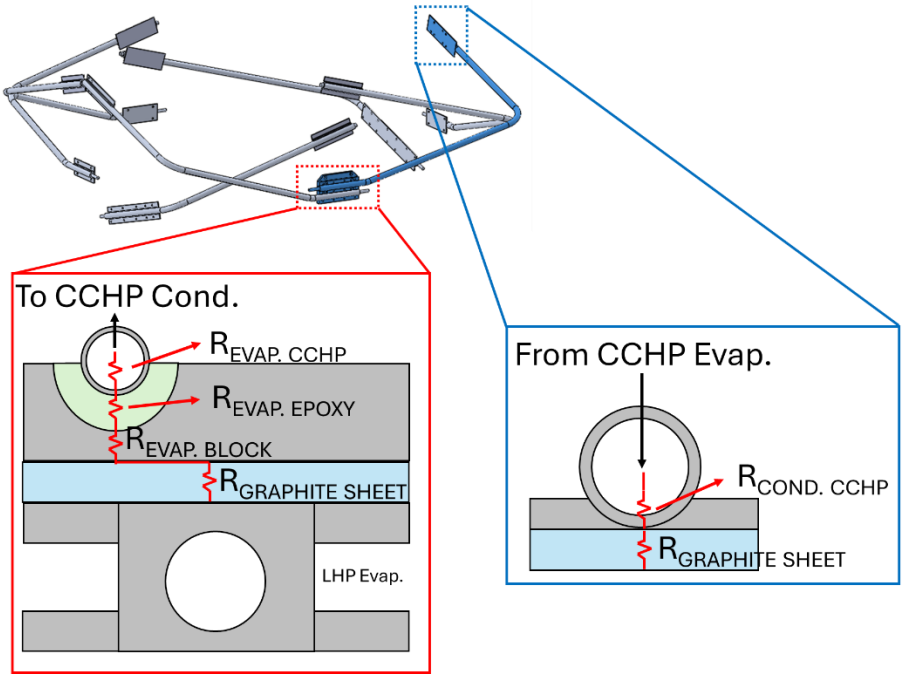

Figure 11. Connecting CCHP Thermal Resistance Network.

Table 1 – Connecting CCHP Thermal Resistance Calculations

Heatpath Resistor Calculator							
Total Resistance	0.58 K/W						
Total Conductance	1.72 W/K						
Total Delta Temp	11.61 K						
Component Name	**Type**	**Area**	**Length**	**Conductance**	**Resistance**	**Power**	**dT**
Grafoil, LHP to E Block	TIM	5 in^2		3 W/in^2/K	0.067 K/W	20 W	1.33 K
Alum CCHP Evap Block	Solid	4 in^2	0.4 in	180 W/m/K	0.022 K/W	20 W	0.44 K
Grafoil, E Block to CCHP	TIM	3 in^2		3 W/in^2/K	0.111 K/W	20 W	2.22 K
CCHP Evaporator	Evap		4 in	2.5 W/in/K	0.100 K/W	20 W	2.00 K
CCHP Condenser	Cond		2.5 in	3.5 W/in/K	0.114 K/W	20 W	2.29 K
Grafoil, CCHP Cond to LHP	TIM	2 in^2		3 W/in^2/K	0.167 K/W	20 W	3.33 K

TESTING

Testing was sub-divided to validate each component or subsystem to facilitate the delivery of TMS components to JSC for rover integration. For example, the warm-box Heat Spreaders were tested and delivered first, as they are required for mounting of electrical components and integrated into the core of the rover very early during the build process. As each sub-system or component was built, the thermal performance was reported in an as-built state to compare to modeling predictions and inform the as-built state of the rover. While testing of all major subcomponents was completed prior to delivery, only the heat spreaders and LHPs are discussed

here. TVAC testing of the integrated Rover TMS, i.e. all subassemblies together, is expected to be completed by NASA in the future prior to launch.

Heat Spreaders

Each heat spreader was tested in a "benchtop setting" individually in earth gravity. The testing was also done in two rounds. First, all panels were tested oriented at 9.6° above horizontal to represent moon gravity. Second, the aft panel itself was tested in a completely vertical orientation to be representative of what will be seen in fully integrated rover testing on earth.

For all tests, the setup was similar. Heat loads representative of each electronic component were simulated with bolted on aluminum plates and adhesive, resistive heaters wired to DC power supplies. The thicknesses of each heater plate was chosen to represent the mounting hardware component flange thickness. The heat rejection provided by the LHP in flight, was represented in testing via an aluminum plate with the same footprint and thickness of the LHP evaporator flange attached to a copper tubed cold plate with a recirculating benchtop chiller utilizing propylene glycol water mixture. Thermal interface material was selected to be flight representative graphite sheet of 0.254 mm thickness. Testing was performed at atmospheric pressure, compared the vacuum environment of flight operation. Each panel was encapsulated in at least 25.4 mm thick closed cell foam to minimize losses. The insulation was evaluated and tracked for parasitic heat leak via a representative test ran on the forward panel. The power applied to each heater plate then accounted for an estimated amount of heat leak. On the heat input side, temperatures were recorded on top of the heater plates in locations corresponding to the expected maximum temperatures based on the thermal gradients seen in the analyses. Thus, the temperature readings could be compared to the component max temperature limits, as they included the interface to the component. Temperatures on the heat rejection side were recorded on the side of the aluminum plate attached to the cold plate, and were thus representative of the LHP evaporator body flange. Thus, each performance test was ran with the goal of adjusting the chiller setpoint until the average of the cold side temperatures was 30°C ± 2.5°C, such that the results could also be compared to the analyses.

All flight representative performance tests ran in the tilted orientation yielded passing results in terms of the component max temperature limits. Additionally, the tests agreed well with the analyses at steady state. Overall, the heat spreader testing highlighted two main items. First, due to the inserts being slightly proud (< 0.127 mm) of the face sheet, it was found that the contact resistance to the component can be dropped relatively significantly by cutting the inserts out of the TIM. In the case of one heater plate, the max temperatures dropped by a full 1°C for 26W of input power after cutting clearance for the inserts out of the TIM. This was later solved on the flight panels by skimming the inserts to be more flush with the face sheets. Second, the CCHPs may see startup transients due to being gravity aided and liquid pooling at the evaporator prior to power application. This effect was seen as sharp inflection points seen in the temperature vs. Time plots. This specific item was investigated further with the completely vertical testing of the aft panel, along with different startup heater configurations to minimize the effects. Figure 12 below shows pictures of the test setup and a plot for the tilted testing of the aft panel. The green lines are for the transceiver heater plate and stabilize at approximately 50°C, followed by the red/blue lines for the motor controllers stabilizing at approximately 40°C, and lastly the purple

lines for the LHP evaporator flange simulator/cold plate. The port heat spreader was tested with temperature measurement on the actual panel face sheets, rather than only the bolted on heater plates or cold plate, and could thus be compared directly to analysis. To this comparison, the results agreed relatively well with temperatures being within 5°C between analysis and testing.

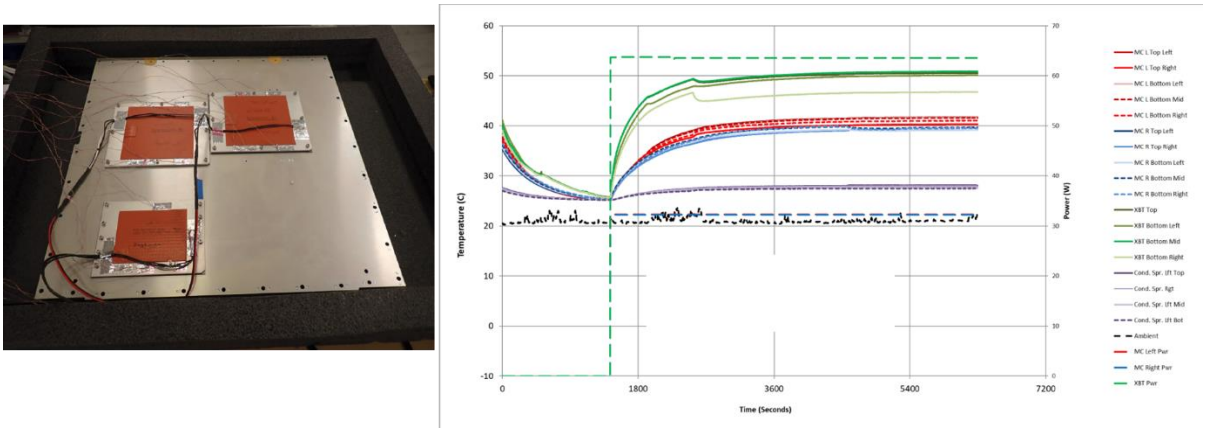

Figure 12. Aft heat spreader testing – plot on the right is time vs. Temperature. Purple is the simulated LHP flange/cold plate, red/blue the motor controller heater plates, and green the transceiver heater plate

LHPs

Each of the four LHPs where tested after charging to ensure consistent and expected behavior during operation. Heat loads were applied directly to the LHP evaporator via an aluminum plate with cartridge heaters. This is different than flight operation, where the heat loads would be applied on the heat spreader to which the LHP is mounted. Heat rejection from the condenser serpentine was done via mounting to an aluminum cold plate, rather than the flight radiator panel, and with grafoil thermal interface material, rather than the flight epoxy. This cold plate approach was taken to allow build and testing of the LHPs prior to receiving the radiators and to minimize risk of damage to the flight radiators which were long lead time and fragile in comparison. This approach also allowed ambient testing for cooling via copper tubing in the cold plate via liquid nitrogen, rather than radiation to space from the radiator panel as in the flight operation. The LHPs with integrated TCVs at the time of testing were mounted to a "mock" warm-box with flight like grafoil under the evaporators. The "mock" warm-box consisted of lightweighted aluminum plates, taking the place of the flight heat spreaders. The entire test set-up, including the transport lines was covered in at least 25.4 mm of closed cell foam insulation to minimize heat leaks during testing.

Conductance of the LHP is defined below which indicates the temperature differential needed to transport the heat input. This is the most conservative approach as the calculation uses the largest temperature gradient.

$$Conductance\left(\frac{W}{K}\right) = \frac{Q}{T_{EVAP,MAX} - T_{COND,MIN}}$$

Each of the four LHPs, indicated by rover mounting orientation, underwent a standard battery of tests to evaluate start up, Hot Op. conductance, and TCV cycling. More in-depth testing was performed on the starboard LHP to characterize the LHP across a larger set of operating conditions. Table 2 summarizes the on-conductance for the 4 LHPs. One can see relatively good agreement with the approximate 20 W/K predicted by the hand calculations during the analysis/design portion of the program.

Table 2 – LHP Conductance at 10°C Condenser

	Conductance (W/K) at 10°C Condenser			
	FORWARD	STARBOARD	AFT	PORT
Test 1	27.5	27.2	26.0	19.6
Test 2	22.2	28.7	30.2	19.7
Test 3	22.6	22.8	33.0	
Test 4	24.2			

The condenser step down testing shown in Figure 13 below shows the TCV turning the LHP conductance off, moving from Hot Op. to Survival. This test consists of a constant heat input into the LHP evaporator along with decreasing the temperature of the condenser in steps via the liquid nitrogen cold plate and a PID controller. The TCV cycled into Survival mode as the evaporator average temperature reached -10°C, causing a slight rebound or increase in the evaporator temperature as the condenser temperature continued to drop indicating successful operation of the TCV. Even with fluctuations in power provided to the evaporator, the evaporator temperature remained the same.

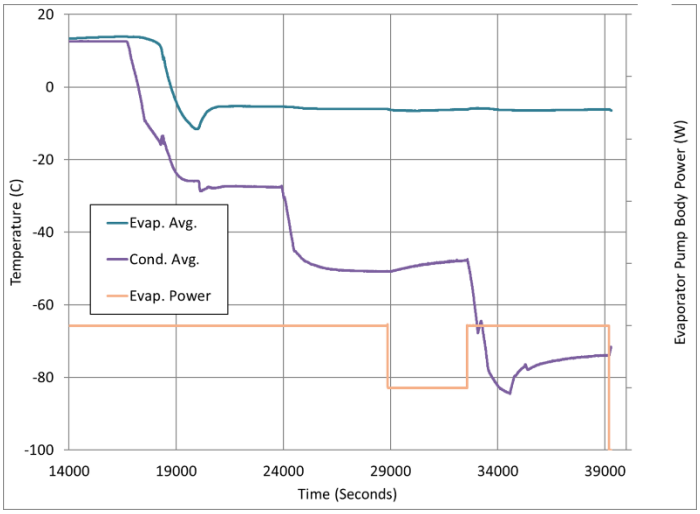

Figure 13. LHP Condenser Step-down testing demonstrating TCV turning conductance off. Blue is LHP evaporator average, purple is LHP condenser average, yellow/gold is LHP evaporator power

Temperature control of the evaporator was demonstrated by applying heat to the compensation chamber of the LHP. Applying heat in this location raises the saturation temperature of the

working fluid in the pump body, causing a rise in operating temperature. A thermostatic controller was used to apply the heat, and temperature control with a simple on-off (bang-bang) controller is shown below. This allows for additional level of control at temperatures above TCV cycling. Figure 14 illustrates this.

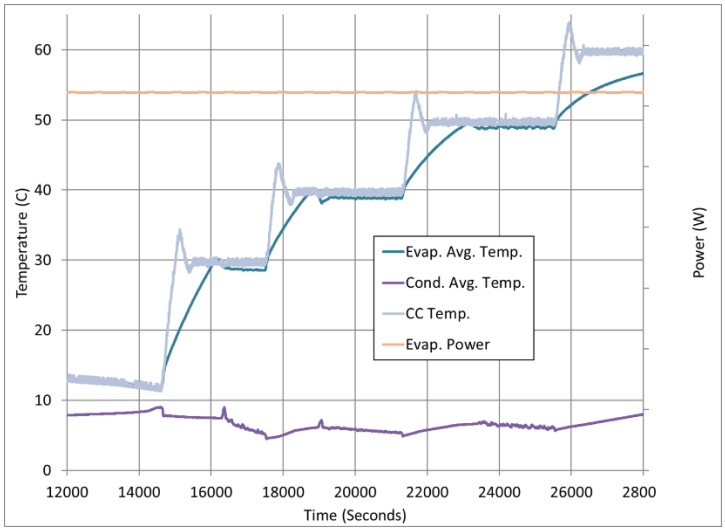

Figure 14. LHP temperature control via applying heat to compensation chamber. Dark blue is LHP evaporator average, light blue is the LHP compensation chamber average, purple is the condenser average temperature, and yellow/gold is the LHP evaporator power.

Conductance was evaluated across a range of heat loads at different operating temperatures. Below in Figure 15 are two selected temperatures for the starboard LHP to highlight difference in performance during Hot Ops (20°C, blue) and Survival (-50°C, orange). Thus, the orange line in Figure 15 is representative of the off-conductance, while the blue line is representative of the on-conductance. Note the values from Table 2 are for 10°C.

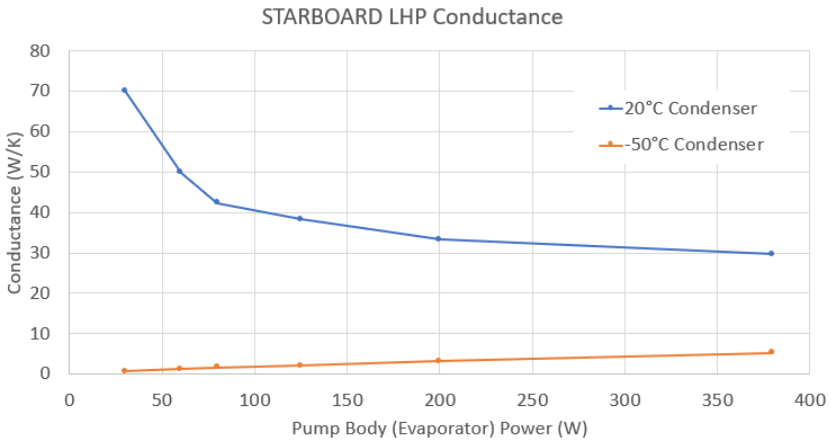

Figure 15. Starboard LHP Conductance during Hot Op. vs. Survival

ACKNOWLEDGEMENTS

This work was completed by Advanced Cooling Technologies, Inc. and funded by the National Aeronautics and Space Administration under Contract No. 80NSSC21C0600. Any opinions, findings, and conclusions or recommendations expressed in this article are those of the authors and do not necessarily reflect the views of the National Aeronautics and Space Administration (NASA). ACT would like to thank Angel Alvarez-Hernandez, Zane Mittag, Jeffrey Hagen, Ezequiel Medici, and Juan Barragan for their support and contributions that supported a successful program.

The authors would like to extend a thanks to all employees at Advanced Cooling Technologies, across all divisions, for the countless contributions and examples of innovation and teamwork required throughout the program.

REFERENCES

[1]Lockhart, R.W. and Martinelli, R.C., "Proposed Correlation of Data for Isothermal Two-Phase, Two-Component Flow in Pipes," *Chemical Engineering Progress*, Vol. 45, 1949, pp. 38-48.